

Time-dependent stresses and curvatures in cracked R.C. sections under working loads

Rajeh Z. Al-Zaid†

Civil Engineering Department, College of Engineering, P.O. Box 800, King Saud University, Riyadh 11421, Saudi Arabia

(Received February 10, 2004, Accepted May 19, 2004)

Abstract. The present study provides a relatively simple and accurate analytical model for the prediction of time-dependent stresses and curvatures of cracked R.C. sections under working loads. A more simplified solution is also provided. The proposed models are demonstrated by considering a numerical example and conducting a parametric study on the effects of relevant R.C. design parameters. In contrary to tension reinforcement, the compression reinforcement is found to contribute significantly in reducing tensile stresses in tension steel and in reducing the total section curvatures. The good accuracy of the proposed approximate solution opens a new vision towards a simple yet accurate model for the prediction of time-dependent effects in R.C. structures.

Key words: cracking; curvatures; reinforced concrete; stresses; time-dependent behavior.

1. Introduction

The determination of the time-varying strains, stresses, and curvatures at critical sections of reinforced concrete (R.C) members is a paramount requisite for their serviceability analysis and design. Creep under sustained loads and shrinkage result in redistribution of strains and stresses between steel and adjoining concrete. Consequently, a continuous change of the depth of neutral axis occurs leading to a time-varying effective compression area and cracking moment. This character is the cause of the complex nature of analysis of R.C. sections under sustained loads.

Several methods for calculating the time-dependent strains and stresses in R.C. members were proposed in the literature (Al-Zaid 2004, Ghali and Favre 1994, Gilbert 1988, Samra 1997, Nie and Cai 2000). The wide-spread used methods include the effective modulus method and the age-adjusted effective modulus method. As initially proposed by Yu and Winter (1960), the effective modulus method replaces the actual concrete modulus with a so-called effective modulus to include the creep and shrinkage effects. The natural gradual change of stresses during the service life of the structure was initially considered by Bazant (1972), who proposed the so-called age-adjusted effective modulus method. Later on, the method was employed for the time-dependent analysis of reinforced and prestressed concrete structures by many researchers, such as Dilger (1982), Ghali (1993), Ghali and Tadros (1985), and Ghali and Favre (1994). The method is simple, but its accuracy is obstructed by

† Associate Professor

the interdependent action of creep and shrinkage where they need to be treated simultaneously, and by the assumption of applicability of the superposition principle particularly after cracking.

The current paper is an extension of the analytical model developed by Al-Zaid (2004), for uncracked sections, to predict strains, stresses and curvatures in cracked R.C. sections under sustained and instant service loads. The model has the merit of being rational yet relatively simple. It is applicable to both cracked and uncracked, rectangular and flanged sections subjected to both axial force and bending moment. It accounts for the movement of the neutral axis with time and the simultaneous action of creep and shrinkage.

2. Model formulation

2.1 Basic assumptions

The basic assumptions made in the proposed model are:

1. Plane sections before deformation remain plane after deformation.
2. Perfect bond exists between reinforcing steel and adjoining concrete.
3. Both concrete and steel obey Hooke's law under service load.
4. Creep is linearly proportions to applied service stress.
5. Shrinkage strain is uniformly distributed over the section.

Throughout this study, compressive forces, stresses and the corresponding deformations are assumed positive. Positive bending moment and curvature are those producing tension in the bottom fibers of a cross section.

A typical R.C. flanged section and the strain distributions at time t_1 when the loads are initially applied and at a later time t are schematically illustrated in Fig. 1.

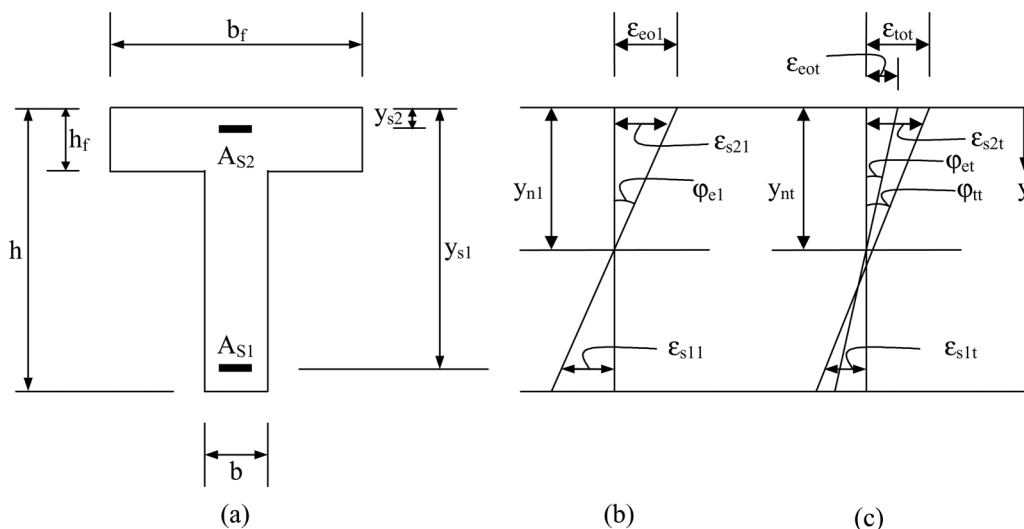


Fig. 1 Reinforced concrete section and schematical illustration for strain distributions: (a) R.C. section, (b) strains at time t_1 , and (c) strains at time t

2.2 Strains and stresses in constituent materials

Consider the strain distributions at times t_1 and t presented in Fig. 1. The elastic and total strains at a specified level of the cross-section are expressed as follows:

$$\begin{aligned}\epsilon_{ey1} &= \epsilon_{eol} - \varphi_{e1}y \\ \epsilon_{eyt} &= \epsilon_{eot} - \varphi_{et}y \\ \epsilon_{tyt} &= \epsilon_{tot} - \varphi_{tt}y\end{aligned}\tag{1}$$

where:

- $\epsilon_{eol}, \epsilon_{eot}$: elastic strains at depth zero (farthest compressed fiber) developed at times t_1 and t , respectively,
- $\varphi_{e1}, \varphi_{et}$: elastic curvatures at times t_1 and t , respectively,
- $\epsilon_{ey1}, \epsilon_{eyt}$: elastic strains at depth y developed at times t_1 and t , respectively,
- $\epsilon_{tot}, \epsilon_{tyt}$: total strains at time t developed at depths zero and y , respectively,
- φ_{tt} : total curvature at time t .

The terms in Eq. (1), prior to the application of live load, are interrelated via the expressions given by Eqs. (2)-(6).

$$\begin{aligned}\epsilon_{tot} &= \epsilon_{eol}(1 + \nu_{1t}) + (\epsilon_{eot} - \epsilon_{eol})(1 + \chi_{1t}\nu_{1t}) + \epsilon_{sh} \\ &= \epsilon_{eot}(1 + \chi_{1t}\nu_{1t}) + \epsilon_{eol}(1 - \chi_{1t})\nu_{1t} + \epsilon_{sh} \\ &= \epsilon_{eot}(1 + \chi_{1t}\nu_{1t}) + c_1 + \epsilon_{sh}\end{aligned}\tag{2}$$

where ν_{1t} and χ_{1t} are the creep and aging coefficients corresponding to the time period $(t - t_1)$, respectively, and ϵ_{sh} is the free shrinkage strain of concrete. The coefficient c_1 is the known creep strain component at time t which is given by,

$$c_1 = \epsilon_{eol}(1 - \chi_{1t})\nu_{1t}\tag{3}$$

At the neutral axis, the initial elastic strain, $\epsilon_{ey_{n1}1}$, is zero. Therefore, the expression of the total strain at the neutral axis, $\epsilon_{ty_{n1}t}$, reduces to,

$$\begin{aligned}\epsilon_{ty_{n1}t} &= \epsilon_{ey_{n1}t}(1 + \chi_{1t}\nu_{1t}) + \epsilon_{sh} \\ &= (\epsilon_{eot} - \varphi_{et}y_{n1})(1 + \chi_{1t}\nu_{1t}) + \epsilon_{sh}\end{aligned}\tag{4}$$

By definition, the total curvature φ_{tt} can be expressed as,

$$\begin{aligned}\varphi_{tt} &= \frac{\epsilon_{tot} - \epsilon_{ty_{n1}t}}{y_{n1}} \\ &= \frac{\epsilon_{eol}(1 + \chi_{1t}\nu_{1t}) + c_1 - (\epsilon_{eot} - \varphi_{et}y_{n1})(1 + \chi_{1t}\nu_{1t})}{y_{n1}} \\ &= \frac{c_1 + \varphi_{et}y_{n1}(1 + \chi_{1t}\nu_{1t})}{y_{n1}}\end{aligned}\tag{5}$$

Eq. (5) can be written in the form,

$$\varphi_{tt} = c_2 + \varphi_{et}(1 + \chi_{1t}v_{1t}) \quad (6)$$

where the coefficient c_2 is the known portion of curvature at time t as given by,

$$c_2 = \frac{c_1}{y_{n1}} = \varphi_{e1}(1 - \chi_{1t})v_{1t} \quad (7)$$

The strain in any steel layer at depth y_{si} developed at time t prior to the application of instant live load, $\varepsilon_{sy_{si}t}$, can be expressed as,

$$\begin{aligned} \varepsilon_{sy_{si}t} &= \varepsilon_{tot} - \varphi_{tt}y_{si} \\ &= c_1 + \varepsilon_{eot}(1 + \chi_{1t}v_{1t}) - [c_2 + \varphi_{et}(1 + \chi_{1t}v_{1t})]y_{si} + \varepsilon_{sh} \\ &= [c_1 - c_2y_{si} + \varepsilon_{sh}] + (\varepsilon_{eot} - \varphi_{et}y_{si})(1 + \chi_{1t}v_{1t}) \end{aligned} \quad (8)$$

Thus, the stress in any steel layer at depth y_{si} , f_{si} , can be expressed as,

$$\begin{aligned} f_{si} &= E_c \frac{E_s}{E_c} [c_1 - c_2y_{si} + \varepsilon_{sh}] + E_c \frac{E_s}{E_c} (1 + \chi_{1t}v_{1t})(\varepsilon_{eot} - \varphi_{et}y_{si}) \\ &= E_c \{n(c_1 - c_2y_{si} + \varepsilon_{sh}) + n'(\varepsilon_{eot} - \varphi_{et}y_{si})\} \end{aligned} \quad (9)$$

where, $n = \frac{E_s}{E_c}$ and $n' = n(1 + \chi_{1t}v_{1t})$

2.3 Equilibrium equations

Consider a concrete section reinforced by a number of steel layers and subjected at any instant of time to an equivalent force-couple system at the farthest compressed fiber of values P and M . The resultant couple M is related to the moment due to the service applied load, M_w , and the axial load, P , by:

$$M = M_w - Pe \quad (10)$$

The eccentricity e of the axial force P is measured from the farthest compressed fiber and is considered positive when downward. To generalize the section analysis, the equilibrium conditions are written in the form,

$$P = C_c + F_{st} \quad (11)$$

$$M = M_c + M_{st} \quad (12)$$

The resultant compressive force in concrete, C_c , and its moment, M_c , about the farthest compressed fiber, $y = 0$, are obtained for the general elastic strain distribution, $\varepsilon_{eyt} = \varepsilon_{eot} - \varphi_{et}y$, by employing the integral equations,

$$C_c = E_c \int_0^D \varepsilon_{eyt} \cdot b(y) dy = E_c (A_c \varepsilon_{eot} - S_c \varphi_{et}) \quad (13)$$

and

$$M_c = -E_c \int_0^D \epsilon_{eyt} \cdot b(y) \cdot y \cdot dy = E_c(-S_c \epsilon_{eot} + I_c \varphi_{et}) \quad (14)$$

where,

- A_c = entire area of concrete section if uncracked or compressed area of concrete section if cracked
- S_c = first moment of area A_c about the reference line $y = 0$
- I_c = moment of inertia of area A_c about the reference line $y = 0$.
- D = an integration limit = h if the section is uncracked, = y_n if cracked.

The total net force in all steel layers available in the section, F_{st} , is given by,

$$F_{st} = E_s \Sigma (c_1 + \epsilon_{sh} - c_2 y_{si}) A_{si} + E_c \Sigma n'_{ei} (\epsilon_{eot} - \varphi_{et} y_{si}) A_{si} \quad (15)$$

where n'_{ei} is the effective modular ratio = n' for steel in cracked concrete, otherwise $n'_{ei} = n' - 1$. Eq. (15) can be written in the form,

$$F_{st} = \bar{F}_{st} + E_c \Sigma n'_{ei} (\epsilon_{eot} - \varphi_{et} y_{si}) A_{si} \quad (16)$$

where \bar{F}_{st} is the known portion of the force F_{st} at time t as given by the first term in Eq. (15).

The moment of F_{st} about the reference line $y = 0$, M_{st} , is given by,

$$M_{st} = -E_s \Sigma (c_1 + \epsilon_{sh} - c_2 y_{si}) A_{si} y_{si} - E_c \Sigma n'_{ei} (\epsilon_{eot} - \varphi_{et} y_{si}) A_{si} y_{si} \quad (17)$$

Eq. (17) can be written in the form,

$$M_{st} = \bar{M}_{st} - E_c \Sigma n'_{ei} (\epsilon_{eot} - \varphi_{et} y_{si}) A_{si} y_{si} \quad (18)$$

where \bar{M}_{st} is the known portion of the moment M_{st} at time t as given by the first term in Eq. (17).

Substituting Eqs. (13) and (16) into Eq. (11) and Eqs. (14) and (18) into Eq. (12) and rearranging the terms lead to the following general equilibrium equations:

$$\bar{P} = E_c [A \epsilon_{eot} - S \varphi_{et}] \quad (19)$$

$$\bar{M} = E_c [-S \epsilon_{eot} + I \varphi_{et}] \quad (20)$$

The solution of Eqs. (19) and (20) for ϵ_{eot} and φ_{et} can be set in the following matrix form:

$$\begin{Bmatrix} \epsilon_{eot} \\ \varphi_{et} \end{Bmatrix} = \frac{1}{AI - S^2} \begin{bmatrix} I & S \\ S & A \end{bmatrix} \begin{Bmatrix} \bar{P} \\ \bar{M} \end{Bmatrix} \frac{1}{E_c} \quad (21)$$

The definitions of the symbols in Eq. (21) depend on whether the section is cracked or uncracked and whether the analysis is for instantaneous or sustained load effects as explained herein.

2.4 Initial strain distribution

The analysis will give the axial elastic strain and curvature at time t_1 , $\left\{ \begin{matrix} \varepsilon_{e01} \\ \varphi_{e1} \end{matrix} \right\}$, immediately after the application of P and M . The solution is obtained from Eq. (21) with the following substitutions:

$$\begin{aligned} \bar{P} &= P \\ \bar{M} &= M \\ A &= bD + A_f + \Sigma n_{ei} A_{si} \\ S &= \frac{bD^2}{2} + S_f + \Sigma n_{ei} A_{si} y_{si} \\ I &= \frac{bD^3}{3} + I_f + \Sigma n_{ei} A_{si} y_{si}^2 \\ D &= h \quad \text{if uncracked} \\ &= y_{n1} \quad \text{if cracked} \\ A_f &= (b_f - b)h_f \\ S_f &= (b_f - b)\frac{h_f^2}{2} \\ I_f &= (b_f - b)\frac{h_f^3}{3} \\ b &= b_f \quad \text{if } y_{n1} \leq h_f \end{aligned} \quad (22)$$

where n_{ei} is the effective modular ratio = n for steel in cracked concrete, otherwise $n_{ei} = n - 1$, and y_{n1} is the depth of neutral axis of the cracked section at time t_1 when the load is initially applied. The depth y_{n1} is obtained from Eq. (21) as follows:

$$y_{n1} = \frac{\varepsilon_{e01}}{\varphi_{e1}} = \frac{IP + SM}{SP + AM}, \quad P \neq 0 \quad (23)$$

$$y_{n1} = \frac{S}{A}, \quad P = 0 \quad (24)$$

Substituting the expressions given by Eq. (22) for A , S and I with $D = y_{n1}$ into Eqs. (23) and (24) and arranging the terms lead to the following equations in y_{n1} :

$$\begin{aligned} y_{n1}^3 + \frac{3M}{P}y_{n1}^2 + \frac{6}{b}\left(S_f + \Sigma n_{ei} A_{si} y_{si} + \frac{M}{P}(A_f + \Sigma n_{ei} A_{si})\right)y_{n1} \\ - \frac{6}{b}\left(I_f + \Sigma n_{ei} A_{si} y_{si}^2 + \frac{M}{P}(S_f + \Sigma n_{ei} A_{si} y_{si})\right) = 0 \quad P \neq 0 \end{aligned} \quad (25)$$

$$y_{n1}^2 + \frac{2}{b}(A_f + \Sigma n_{ei} A_{si})y_{n1} - \frac{2}{b}(S_f + \Sigma n_{ei} A_{si} y_{si}) = 0 \quad P = 0 \quad (26)$$

2.5 Strain distribution at time t

2.5.1 Prior to the application of live load

The axial elastic strain and curvature at time t after the sustained load effects have occurred and prior to the application of live load, $\left\{ \begin{matrix} \varepsilon_{eot} \\ \varphi_{et} \end{matrix} \right\}$, are obtained from Eq. (21) with the following substitutions:

$$\bar{P} = P - \bar{F}_{st} \tag{27}$$

$$\bar{M} = M - \bar{M}_{st} \tag{28}$$

$$A = bD + A_f + \Sigma n'_{ei} A_{si}$$

$$S = \frac{bD^2}{2} + S_f + \Sigma n'_{ei} A_{si} y_{si}$$

$$I = \frac{bD^3}{3} + I_f + \Sigma n'_{ei} A_{si} y_{si}^2$$

$$D = h \quad \text{if uncracked}$$

$$= y_{nt} \quad \text{if cracked}$$

$$b = b_f \quad \text{if } y_{nt} \leq h_f \tag{29}$$

where y_{nt} is the depth of neutral axis at time t which is obtained from Eq. (21) as follows:

$$y_{nt} = \frac{\varepsilon_{eot}}{\varphi_{et}} = \frac{\bar{I}\bar{P} + \bar{S}\bar{M}}{\bar{S}\bar{P} + \bar{A}\bar{M}} \tag{30}$$

Substituting the expressions given by Eq. (29) for A , S and I into Eq. (30) and arranging the terms lead to the following cubic equation in y_{nt} :

$$y_{nt}^3 + \frac{3\bar{M}}{\bar{P}} y_{nt}^2 + \frac{6}{b} \left(S_f + \Sigma n'_{ei} A_{si} y_{si} + \frac{\bar{M}}{\bar{P}} (A_f + \Sigma n'_{ei} A_{si}) \right) y_{nt} - \frac{6}{b} \left(I_f + \Sigma n'_{ei} A_{si} y_{si}^2 + \frac{\bar{M}}{\bar{P}} (S_f + \Sigma n'_{ei} A_{si} y_{si}) \right) = 0 \tag{31}$$

To avoid the difficulty of solving a cubic equation to determine the neutral axis depth y_{nt} at time t , an approximate solution can be obtained by assuming the initial strain distribution (thus the effective compressed area of the cracked section) is unchanged due to creep and shrinkage. With this simplifying assumption, the depth y_{nt} of the compressed concrete area is approximately determined using the following equation:

$$y_{nt} = \frac{A_c \cdot y_c + \Sigma n'_{ei} A_{si} y_{si} + \bar{P} (E_c \varphi_{e1})^{-1}}{A_c + \Sigma n'_{ei} A_{si}} \leq h \tag{32}$$

where A_c is the area of the compressed concrete area of depth y_{n1} and y_c is its centroidal distance measured from the reference line $y = 0$. Once y_{nt} is determined, the geometric properties of the section are calculated using Eq. (29), then the strain distribution is obtained using Eq. (21).

2.5.2 Analysis for live load effect

If at time t , an equivalent live force-couple system P_L and M_L is applied at the extreme compressed fiber, the strain distribution will change to maintain the overall equilibrium of forces and moments. Let $\Delta\varepsilon_{eol}$ denotes the change in strain due to live load at $y = 0$ and $\Delta\phi_{eL}$ denotes the change in the curvature. The analytical model can be used to obtain the change in strain distribution due to live load via the expression,

$$\begin{Bmatrix} \Delta\varepsilon_{eol} \\ \Delta\phi_{eL} \end{Bmatrix} = \frac{1}{AI - S^2} \begin{bmatrix} I & S \\ S & A \end{bmatrix} \begin{Bmatrix} \bar{P} \\ \bar{M} \end{Bmatrix} \frac{1}{E_c} - \begin{Bmatrix} \varepsilon_{eot} \\ \phi_{et} \end{Bmatrix} \quad (33)$$

In Eq. (33), A , S , and I are calculated using Eq. (22) and \bar{P} and \bar{M} are calculated using the following equations:

$$\bar{P} = \Sigma P - \bar{F}_{SL} \quad (34)$$

$$\bar{M} = \Sigma M - \bar{M}_{SL} \quad (35)$$

in which

$$\bar{F}_{SL} = \bar{F}_{st} + E_s \cdot \chi_{1t} \nu_{1t} \Sigma (\varepsilon_{eot} - \phi_{et} y_{si}) A_{si} \quad (36)$$

$$\bar{M}_{SL} = \bar{M}_{st} - E_s \chi_{1t} \nu_{1t} \Sigma (\varepsilon_{eot} - \phi_{et} y_{si}) A_{si} y_{si} \quad (37)$$

The live load effect can also be approximately determined by assuming that the depth of the effective compressed area obtained at time t prior to the application of live load is unchanged. With this assumption, the geometric properties in Eq. (33) are calculated using Eq. (22) with $y_{n1} = y_{nt}$ as calculated from,

$$y_{nt} = \frac{\varepsilon_{eot}}{\phi_{et}} \leq h \quad (38)$$

3. Application of the model

3.1 Numerical example

3.1.1 General

The T-section with dimensions and reinforcement shown in Fig. 2(a) has been analyzed by Ghali and Favre (1994), using the age-adjusted-effective modulus method. To avoid hampering the validity of the principle of superposition utilized by the method, the effective compressed area of the cracked section was assumed to be unchanged due to creep and shrinkage. Since the proposed model takes into account the change in the effective area of concrete by allowing the movement of neutral axis, the numerical example will provide, beside demonstration of the model, the size of error resulting from such an assumption. The input data to the model is as follows:

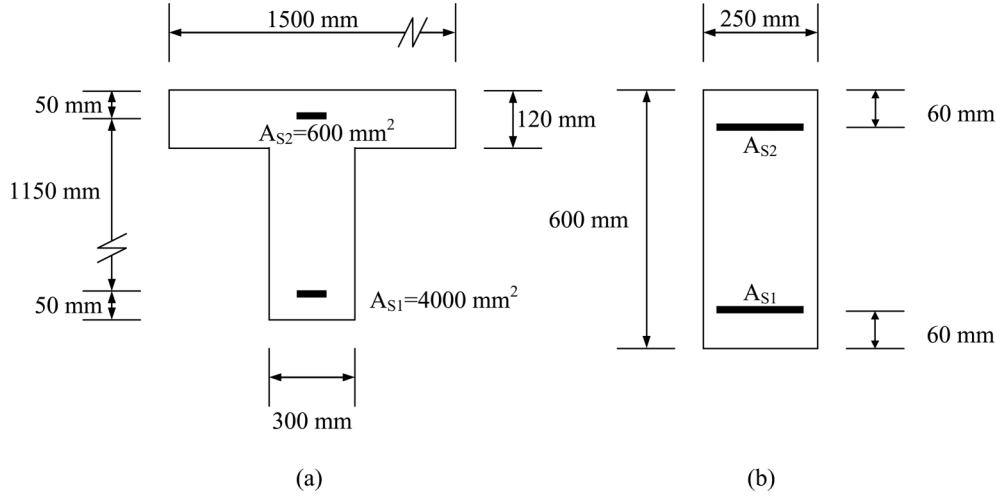


Fig. 2 Reinforced concrete sections used for model illustration

$$E_c = 30 \text{ GPa}, \quad E_s = 200 \text{ GPa}, \\ n = 6.67, \quad \nu = 2.5, \quad \chi = 0.75, \quad \varepsilon_{sh} = 300 * 10^{-6}, \quad n' = 19.18$$

The section is subjected to an axial load $P = 800 \text{ kN}$ at $e = 1000 \text{ mm}$ from the farthest compressed fiber and a bending moment due to service sustained load $M_w = 1000 \text{ kN.m}$. The equivalent force couple system at the farthest compressed fiber becomes,

$$P = 800 \text{ kN}, \text{ and } M = M_w - P.e = 200 \text{ kN.m}$$

The section is assumed to be precracked by setting the modulus of rupture $f_r = 0$.

3.1.2 Analysis at time t_1

The input data given above together with the section dimensions, reinforcement areas and their locations from Fig. 2(a) can be used to determine the coefficients in Eq. (25) which can then be solved for y_{n1} , the height of the compressed area, to get,

$$y_{n1} = 444.6 \text{ mm}$$

The geometric properties of the section are then computed using Eq. (22). Substituting in Eq. (21) and solving for ε_{e01} , the initial strain at the extreme compressed fiber, and φ_{e1} , the initial curvature, give:

$$\varepsilon_{e01} = 179 * 10^{-6} \quad \varphi_{e1} = 0.403 * 10^{-6} \text{ mm}^{-1}$$

Stress at the top fiber, $f_{c1} = 30 * 10^3 * 179 * 10^{-6} = 5.37 \text{ MPa}$

Stress in compression steel, $f_{s21} = 200 * 10^3 [179 - 403 * 50] * 10^{-6} = 31.77 \text{ MPa}$

Stress in bottom steel, $f_{s11} = 200 * 10^3 [179 - 0.403 * 1200] * 10^{-6} = -60.9 \text{ MPa}$

3.1.3 Analysis at time t

Eqs. (3) and (7) can respectively be used to get,

$$\begin{aligned} c_1 &= 179 * 10^{-6} (1 - 0.75) * 2.5 = 111.875 * 10^{-6} \\ c_2 &= 0.403 * 10^{-6} (1 - 0.75) * 2.5 = 0.252 * 10^{-6} \text{ mm}^{-1} \end{aligned}$$

Eqs. (27) and (28) can respectively be used to get,

$$\begin{aligned} \bar{P} &= 800 - 200[(111.875 + 300) * 4600 - 0.252(600 * 50 + 4000 * 1200)] * 10^{-6} \\ &= 664.5 \text{ kN} = 664.5 * 10^3 \text{ N} \\ \bar{M} &= 200 + 200[411.875(600 * 50 + 4000 * 1200) - 0.252(600 * 50^2 + 4000 * 1200^2)] * 10^{-9} \\ &= 307.5 \text{ kN.m} = 307.5 * 10^6 \text{ N.mm} \end{aligned}$$

The coefficients in Eq. (31) can then be determined, hence the equation can be solved to get,

$$y_{nt} = 591.5 \text{ mm}$$

The geometric properties of the transformed section are computed using Eq. (29). Substituting into Eq. (21) and solving for ϵ_{eot} , the elastic strain at the extreme compressed fiber after the creep and shrinkage effects have occurred, and the corresponding curvature ϕ_{et} , give,

$$\epsilon_{eot} = 148.4 * 10^{-6}, \quad \phi_{et} = 0.251 * 10^{-6} \text{ mm}^{-1}$$

Eqs. (2) and (6) are respectively used to get ϵ_{tot} , the total strain at the extreme compressed fiber, and ϕ_{tt} , the total curvature,

$$\epsilon_{tot} = 838.5 * 10^{-6}, \quad \phi_{tt} = 0.974 * 10^{-6} \text{ mm}^{-1}$$

The stresses in concrete and steel will be,

$$\begin{aligned} f_{ct} &= 30 * 10^3 * 148.4 * 10^{-6} = 4.45 \text{ MPa} \\ f_{s2t} &= 200 * 10^3(838.5 - 0.974 * 50) * 10^{-6} = 158 \text{ MPa} \\ f_{s1t} &= 200 * 10^3(838.5 - 0.974 * 1200) * 10^{-6} = -66.1 \text{ MPa} \end{aligned}$$

Alternatively, y_{nt} can approximately be computed using Eq. (32) to get,

$$y_{nt} = 509 \text{ mm}$$

Following the same steps as in the analytical model leads to,

$$\begin{aligned} \epsilon_{eot} &= 149 * 10^{-6}, & \phi_{et} &= 0.25 * 10^{-6} \text{ mm}^{-1}, & y_{nt} &= 596 \text{ mm} \\ \epsilon_{tot} &= 840 * 10^{-6}, & \phi_{tt} &= 0.97 * 10^{-6} \text{ mm}^{-1} \\ f_{ct} &= 4.47 \text{ MPa}, & f_{s2t} &= 158.3 \text{ MPa}, & f_{s1t} &= -64.8 \text{ MPa} \end{aligned}$$

The results obtained using the proposed analytical and approximate models are compared with those obtained using the age-adjusted effective modulus method (Ghali and Favre 1994) in Table 1.

Table 1 Comparison of the results from the numerical example with the results using the age-adjusted effective modulus method

Method of analysis	Initial stresses (MPa)			Stresses at time t (MPa)			Depth of neutral axis (mm)	
	f_{c1}	f_{s21}	f_{s11}	f_{ct}	f_{s2t}	f_{s1t}	y_{n1}	y_{nt}
Proposed analytical model	5.37	31.8	-60.9	4.45	158	-66.1	444.6	591.5
Proposed approximate model	5.37	31.8	-60.9	4.47	158.3	-64.8	444.6	596
Age-adjusted effective modulus method	5.38	31.8	-60.8	4.49	159	-63.8	444	603

3.2 Effect of design parameters

The rectangular section with dimensions and reinforcement locations shown in Fig. 2(b) is considered. The investigation will provide evaluations of the effects of prevalent design parameters on the time-dependent stresses, and on the accuracy of the proposed approximate solution. The design parameters include the following: a) The ratio of live load to dead (sustained) load, L/D , b) The tension reinforcement ratio, ρ , c) The concrete compressive strength, f'_c , and d) The ratio of compression to tension reinforcement, ρ'/ρ . For this purpose, a computer program that implements the proposed models is prepared. The creep coefficient ν , the aging coefficient χ , the shrinkage strain ϵ_{sh} , and the steel modulus of elasticity E_s are kept constant with values 2.5, 0.8, 400 μ , and 200 GPa, respectively.

The output of the computer program is presented in Figs. 3 to 6 in forms of variations of the ratios of stresses and total curvatures at time t to initial stresses and curvatures with the design

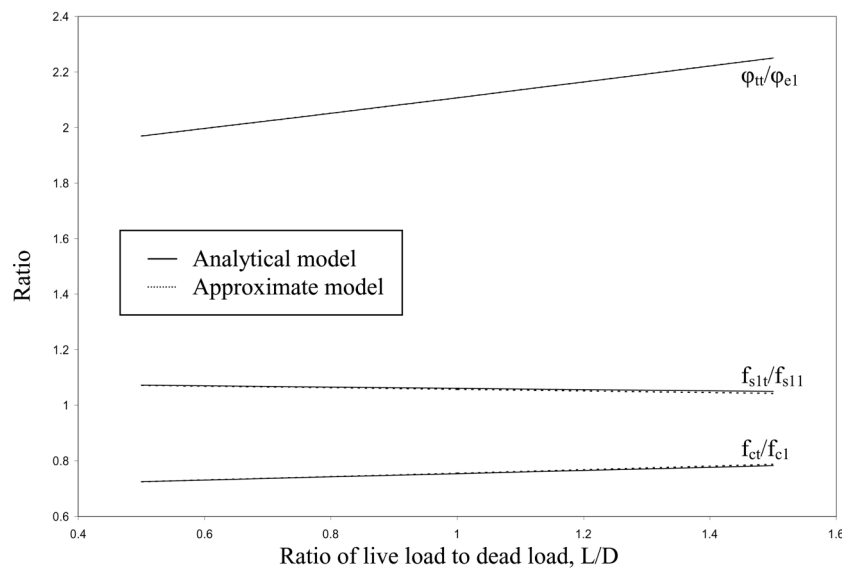


Fig. 3 Effect of live load to dead load ratio

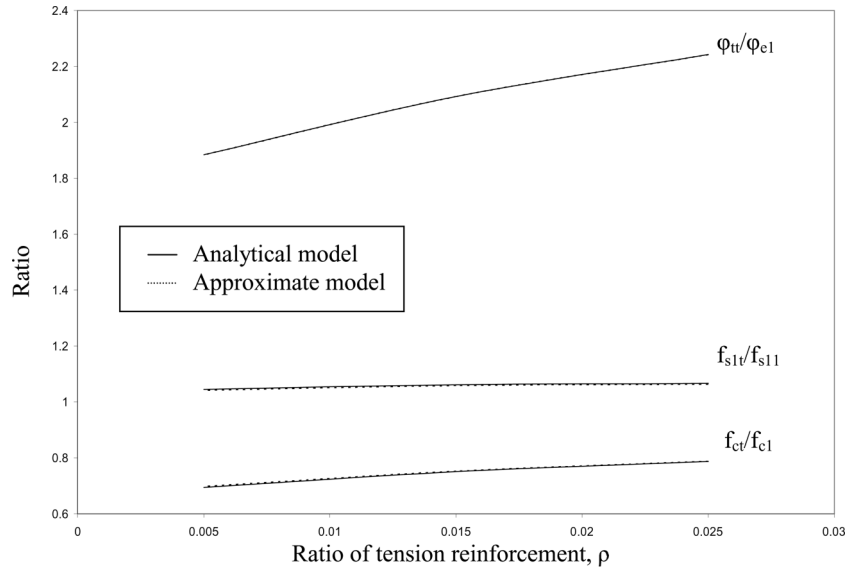


Fig. 4 Effect of tension reinforcement

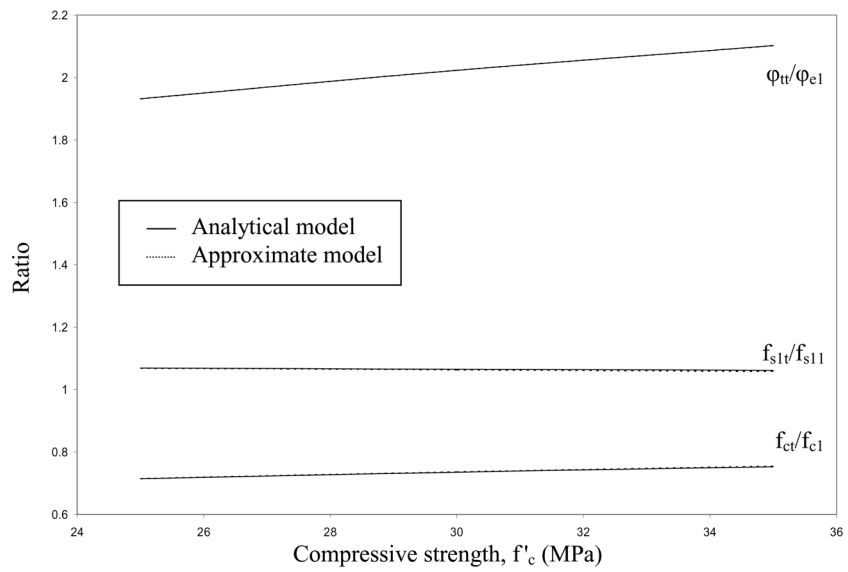


Fig. 5 Effect of compressive strength

parameter under consideration. It is to be noted that for the particular problem, the initial stresses are the same for both the analytical model and the approximate solution. The section design is done according to the flexural strength requirements of the ACI 318-95 code. When varying the compression steel ratio to produce Fig. 6, the sustained moment, M_w , and the axial load, P , are kept constants at 150 kN.m and 500 kN.

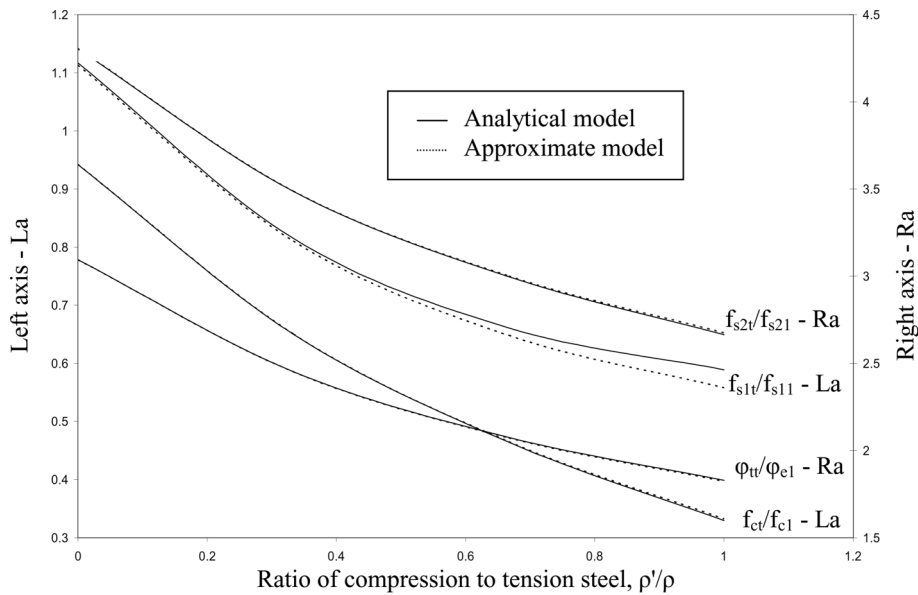


Fig. 6 Effect of compression reinforcement

4. Conclusions

The objective of the present study was to develop a relatively simple and accurate analytical model to predict the time-dependent stresses and curvatures of cracked R.C. sections under working loads. The model takes into account the simultaneous action of creep and shrinkage and their effect on the movement of neutral axis, and the presence of both bending moment and axial force. A more simplified approximate version of the model was established.

The applicability of the model and the accuracy of the simplified approximate solution were demonstrated by considering a numerical example and conducting a parametric study on the effects of relevant design parameters on the model output.

The results of the numerical example presented in Table 1 and those of the parametric study plotted in Figs. 3 to 6, set forth the following trends of time-dependent behavior of R.C. sections:

1. In general, the restraint of creep and shrinkage deformations by reinforcing bars tends to reduce the compressive stresses induced in concrete by applied loads. This effect is more pronounced in sections designed for low L/D ratios (see Fig. 3), and in sections with high ratios of compression reinforcement (see Fig. 6). Such a trend is rationalized by the more creep deformations under high sustained load and by the more restraint provided by the high amount of compression reinforcement.
2. Fig. 6 also shows the significant contribution of the compression reinforcement in reducing the tensile stresses in tension reinforcement and the total section curvature. These reductions approach 35% in tension steel stresses and 40% in curvatures at $\rho'/\rho = 1$. Furthermore, Fig. 6 reveals a significant increase of stresses in compression steel due to creep and shrinkage particularly at low ρ'/ρ ratios.

3. In contrary to compression reinforcement, increasing the amount of tension reinforcement tends to increase the total curvature by about 18% at $\rho = \rho_{max}$ (see Fig. 4). The tension steel effect on stresses is moderate.
4. The effect of f'_c is incorporated in the model by the modular ratio, n , which is proportional to the square root of f'_c . This is behind the moderate effect of the compressive strength of concrete, f'_c , on the stress redistribution between steel and concrete and on total curvature as revealed by Fig. 5.
5. In general, all the figures show the good accuracy of the approximate solution in comparison with the analytical model. This observation opens a new vision towards a reasonably simple solution which provides good predictions of the time-dependent effects in R.C. sections.

References

- ACI Committee 318 (1995), "Building code requirements for structural concrete (ACI 318-95)", American Concrete Institute, Farmington Hills, Michigan, 351 pp.
- Al-Zaid, R.Z. (2004), "Long-term flexural cracking of reinforced concrete members", *Struct. Eng. Mech., An Int. J.*, **17**(1), 15-27.
- Bazant, Z.P. (1972), "Prediction of concrete creep effects using age-adjusted effective modulus method", *ACI J.*, **69**(4), 212-217.
- Dilger, W.H. (1982), "Creep analysis of prestressed concrete structures using creep-transformed section properties", *PCI J.*, **27**(1), 98-118.
- Ghali, A. (1993), "Deflection of reinforced concrete members: A critical review", *ACI Struct. J.*, **90**(4), 364-373.
- Ghali, A. and Favre, R. (1994), *Concrete Structures: Stresses and Deformations*, E&FN Spon, London, 444 pp.
- Ghali, A. and Tadros, M.K. (1985), "Partially prestressed concrete structures", *J. Struct. Eng., ASCE*, **111**(8), 1846-1865.
- Gilbert, R.I. (1988), *Time Effects in Concrete Structures*, Elsevier Sciences Publishing Inc., Amsterdam, 321 pp.
- Nie, Jianguo and Cai, C.S. (2000), "Deflection of cracked RC beams under sustained loading", *J. Struct. Eng., ASCE*, **126**(6), 708-716.
- Samra, R.M. (1997), "Renewed assessment of creep and shrinkage effects in reinforced concrete beams", *ACI Struct. J.*, **94**(6), 745-751.
- Yu, W.W. and Winter, G. (1960), "Instantaneous and long-time deflections of reinforced concrete beams under working loads", *ACI J.*, **57**(1), 29-50.